

# Gaussian mixture models and the population synthesis of radio pulsars

A.P. Igoshev<sup>1\*</sup> and S.B. Popov<sup>2†</sup>

<sup>1</sup> Sobolev Institute of Astronomy, Saint Petersburg State University, Universitetsky prospekt 28, 198504, Saint Petersburg, Russia

<sup>2</sup> Sternberg Astronomical Institute, Lomonosov Moscow State University, Universitetsky prospekt 13, 119991, Moscow, Russia

## ABSTRACT

Recently, Lee et al. used Gaussian mixture models (GMM) to study the radio pulsar population. In the distribution of normal pulsars in the  $P - \dot{P}$  plane, they found four clusters. We develop this approach further and apply it to different synthetic pulsar populations in order to determine whether the method can effectively select groups of sources that are physically different. We check several combinations of initial conditions as well as the models of pulsar evolution and the selection effects. We find that in the case of rapidly evolving objects, the GMM is oversensitive to parameter variations and does not produce stable results. We conclude that the method does not help much to identify the sub-populations with different initial parameters or/and evolutionary paths. For the same reason, the GMM does not discriminate effectively between theoretical population synthesis models of normal radio pulsars.

**Key words:** methods: statistical, pulsars: general, X-rays: binaries, gamma-ray burst: general

## 1 INTRODUCTION

While radio pulsars are known for more than 45 years (Hewish et al. 1968), many aspects of their initial properties and the evolution are not well understood. The evolution of a pulsar is a long process and cannot be studied directly. Fortunately, about 2000 pulsars at different stages of their evolution are currently being observed (Manchester et al. 2005). Therefore, since the early seventies, different methods of statistical analysis of the radio pulsar population and its evolution have been proposed (see Vivekanand & Narayan 1981; Vranesević & Melrose 2011 and references therein). The latest attempt was made by Lee et al. (2012) (hereafter L12).

These authors use a Gaussian mixture model (GMM) to identify groups of pulsars in the  $P - \dot{P}$  plane. In this approach, it is assumed that the density of objects inside a group (a cluster) can be fitted with a two-dimensional normal distribution (in linear or logarithmic scale). Here, we develop further the approach used by L12<sup>1</sup>. We analyse the distributions in the space of periods and period derivatives, both on logarithmic scale. In other words, the sources belonging to every cluster have log-gaussian distribution. In the plots below, these groups of sources are represented by  $2\text{-}\sigma$  contours, and we call them ellipses, which actually stands for “a group selected by the GMM with log-gaussian distribution of density of objects in both coordinates”.

We are interested in understanding the origin of the clusters

found by L12 for normal radio pulsars, as well as in checking if the GMM can be used to differentiate between different population synthesis calculations. We present the analysis of several toy models with well-understood properties, provide an additional analysis of the observed population of the radio pulsars, and finally, apply the cluster analysis to study the realistic synthetic sets of the data produced by the advanced population synthesis models.

The paper is organized as follows. In the next section we briefly describe the GMM method. In Section 3, the GMM method is applied to different pulsar populations — both, synthesized and observed. Our population synthesis models and calculations are also presented in the third Section. In Section 4, we discuss the effectiveness of the GMM method to falsify theoretical population synthesis models and present two examples of the application of this method to other sets of sources. Finally, we present our conclusions.

## 2 GAUSSIAN MIXTURE MODEL

The GMM is an iterative method which allows one to find clusters of objects that follow the Gaussian distribution. Each set of the clusters describes the data with some probability. We are interested in finding the one which gives a higher probability for a smaller number of clusters.

The GMM as an unsupervised learning algorithm has demonstrated its efficiency in different areas where it used to extract empirical knowledge from data samples (Kim & Kang 2007; Reynolds et al. 2000). Note that Gaussians on which the method is

\* E-mail: ignotur@gmail.com

† E-mail: sergepolar@gmail.com

<sup>1</sup> We thank Kejia Lee for providing the original code used in the study L12

based are not basis functions. Nevertheless, the central limit theorem may be used to explain our motivation to use this method. Indeed, a position of a pulsar in the  $P - \dot{P}$  plane is a two-dimensional independent random variable because it is determined by the effective magnetic field and the age. The logarithm of the effective magnetic field is in the range [10, 13], and the logarithm of the age is in the range [3, 10]<sup>2</sup>. This defines a rather narrow variance range. The central limit theorem states that a set of the large number of independent random variables where every variable belongs to a distribution with similar mean and variance has limiting distribution function approaching the normal distribution. This is our main motivation to use Gaussians to study the pulsar distribution.

All calculations start with only one cluster. We then probe sequentially  $\sim 20$  different initial positions of a cluster which cover the entire data range. It is found that the size of the initial cluster does not change the results, while the position of the initial cluster is crucial. At the next step, we maximize the likelihood by varying the model parameters. The details of the procedure of likelihood maximization, which is called below the Expectation-Maximization algorithm (Press et al. 2007) are described in detail in L12. This procedure is run for all initial guesses for one cluster. As a result, we have a few (typically 4-5 out of 20) sets of cluster parameters with significantly different properties. For each of them we generate 10 samples of data points, and for each such sample we carry out the two-dimensional Kolmogorov-Smirnov (K-S) test. The most probable set of cluster parameters is used later as a fixed initial guess for the first cluster. Now, we add the second cluster. For the second cluster, we also make 20 initial guesses. The Expectation-Maximization algorithm is run, and finally, after application of the K-S test, we fix the initial guess for both clusters (note, that the initial guess for the first cluster could change when we analyse a two-cluster model). Following this algorithm we find all sets of cluster parameters sequentially from one cluster to some maximum number of clusters.

Up to this moment we do not exclude any significantly distinct sets of clusters. When all final sets of clusters (in our study up to 4-5 clusters in each set) are found, we again generate 20 samples of data points.

In our numerical experiments, we found that if we use sets with more than 5 clusters then we obtain a large number of different solutions with equally high probabilities (this is called overfitting in L12). On the other hand, when we limit the number of clusters to 4-5, we typically obtain no more than one or two solutions with comparably high probabilities.

We compare these samples to each other by means of the K-S test, and then study the distribution of  $D$ 's (this is the Kolmogorov-Smirnov statistic).

Finally, we calculate the probability that the data are drawn from the synthetic sample which corresponds to the chosen set of clusters, and the analysed data (observed or obtained by a population synthesis model) are drawn from the same parent distribution based on the mean value of  $D$  for the analyzed data.

As the final result we select the set of clusters which has the highest probability (higher than  $\sim 90$  per cent) and which contains the smallest number of clusters. As it is mentioned in L12, the cumulative distribution for the two-dimensional K-S test is not well defined. Due to this, it was suggested to compute a cumulative distribution of  $D$  for every model, and then we rely on this numerical

statistics when we calculate the probability. Based on our experience such numerical cumulative distribution does not provide better resolution than about a few percent. We say that the probability is 99.9 per cent when  $D$  lies to the left from the beginning (the first data point) of the cumulative distribution, i.e. in the region where our simulation does not have enough resolution.

### 3 GMM FOR DIFFERENT POPULATIONS

In this section we present the cluster analysis using the Gaussian mixture model for several synthetic and observed populations of normal radio pulsars.

First, we study the same population as in L12 to be certain that we can reproduce their results. Once we have made sure that this is indeed the case, we apply the method to other populations: the observed and the synthetic one.

In all cases, for a given set of the data points in the  $P - \dot{P}$  plane (observed or calculated) several runs of the Expectation-Maximization algorithm are made for different sets of initial guesses (see details in L12). These runs produce different sets of the Gaussian ellipses (the number of ellipses can also be different) which describe the data with some probability defined according to the multi-dimensional Kolmogorov-Smirnov test. Typically, we try to use as small a number of ellipses as possible to describe the data with a reasonable probability, and we demonstrate only one plot with the largest probability for the given number of ellipses.

When a distribution of pulsars is analysed, the GMM method provides multiple solutions, and to choose the most appropriate one it is necessary to use some formal criteria. We use the K-S test probability as such formal parameter. Some sets of ellipses which do not have as high probability as the presented ones, potentially can reflect physically linked groups of pulsars better. However, since *a priori* we do not have enough information, it is possible that we can miss such good solutions.

#### 3.1 Analysis of observed populations

L12 made their analysis for a mixed population where, in addition to normal radio pulsars, sources like magnetars and close-by cooling radio quiet neutron stars (NSs) were also considered. We exclude those objects which have been initially identified not as radio pulsars, but as sources of a different nature (magnetars, rotating radio transients, cooling near-by NSs, etc.). Results are shown in Figure 1. We present two most probable realisations based on the same data set.

As in L12, four clusters are necessary to describe the data. First, let us note that both pictures are different from the one in L12. As we removed from the data most of the sources with large  $P$  and  $\dot{P}$  (upper right part of the diagram: all magnetars and close-by cooling NSs) the ellipse corresponding to this part of the diagram in L12 is changed. However, this is not the only modification. This is especially obvious in the left panel of Figure 1, which has a higher probability: in this plot one of the ellipses is shifted towards the region with smaller  $\dot{P}$  with respect to the figure in L12. Only the ellipse lying along the death line saves its position. In our opinion, this argues against the effectiveness of the method to identify physically or evolutionary related groups of normal radio pulsars.

We also tried to check what happens if the set of the pulsars considered is slightly modified. We randomly excluded 10 per cent of the sources (Figure 2). Again, we see that the results are changed.

<sup>2</sup> Here it is reasonable to consider logarithms of quantities because we apply the GMM in the logarithmic scale.

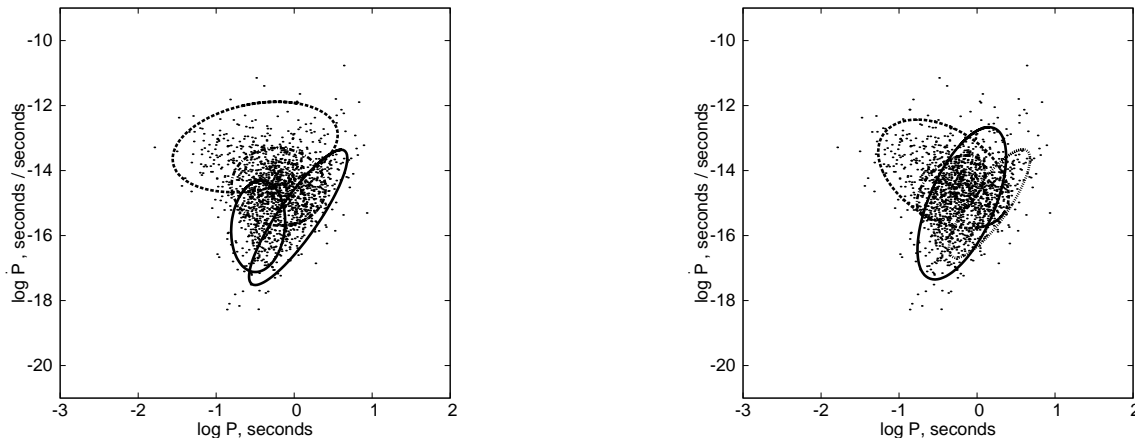


**Figure 1.**  $P - \dot{P}$  diagram for normal pulsars with ellipses derived with the GMM. No magnetars, rotating radio transients, cooling near-by NSs, etc. are included into the data set. The probability that the model and the data are drawn from the same parent distribution is 98 per cent for the model in the left panel, and 95 per cent for the model in the right panel.

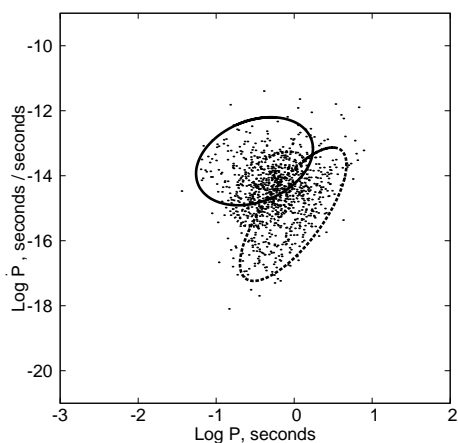


**Figure 3.** The Parkes multibeam survey pulsars and the related clusters identified with the GMM. The number of data points is 905. The probability that the model and the data are drawn from the same parent distribution is 94 per cent.

In one (left) plot we obtained close to a carbon-copy of the distribution from L12, though magnetars are excluded here. In another, which has a very similar probability, high-B pulsars do not form a separate group (note, that the data are the same, only the initial combination of the ellipses is different).

Finally, we take only 905 pulsars detected in the Parkes multibeam survey (Manchester et al. 2001) to get rid of some of the selection effects (Figure 3). The picture is now simplified and becomes more stable. One three ellipses are required. One is most probably related to the existence of the death line. To see if we can find interpretations for the others we run several population synthesis models with different assumptions.

### 3.2 Toy models of the pulsar evolution

One of the main tasks of this study is to try to understand the origin of the clusters found for the observed populations. To do this in a systematic manner we perform several runs for different synthetic populations based on well-understood assumptions with regards to their evolution, the spatial distribution, etc. We use population syn-

thesis models of different complexity to see if an addition of a new option (for example, the field decay or the Galactic spiral structure) produces a new cluster or even changes the whole picture.

Let us briefly describe the basic features of our population synthesis models. Typically, pulsars are born in four spiral arms (unless the opposite is explicitly stated). The spiral arms are parametrized according to Vallée (2005). The initial spin periods are taken from the Gaussian distribution with  $\langle P_0 \rangle = 0.3$  s and  $\sigma_p = 0.15$  s. The initial magnetic fields are described by the Gaussian distribution in log-scale:  $\langle \log B_0 / [\text{G}] \rangle = 12.65$  and  $\sigma_B = 0.55$  (if opposite is not explicitly stated). Pulsars are born with constant rate, the oldest have ages of  $3 \cdot 10^8$  years.

The motion of every pulsar in the Galaxy is determined by its birth place, the kick velocity, and the Galactic gravitational potential. In all models we use the potential proposed by Kuijken & Gilmore (1989). The kick velocity distribution is chosen in the form:

$$p(v_l) = \frac{1}{2\langle v_l \rangle} \exp \left[ -\frac{|v_l|}{\langle v_l \rangle} \right]. \quad (1)$$

Here  $\langle v_l \rangle = 180 \text{ km s}^{-1}$  (Faucher-Giguère & Kaspi 2006);  $|v_l|$  denotes the absolute value of  $v_l$ . Every component of the velocity vector is determined according to the probability defined by Equation (1). We neglect the Shklovskii effect as well as the changes of the relative position of the Sun and the spiral arms.

A pulsar is “detected” if its luminosity exceeds the limit  $S_{\text{min}}$  for the Parkes multibeam survey (Manchester et al. 2001). The radio luminosity is calculated as (Faucher-Giguère & Kaspi 2006):

$$\log L = \log(L_0 P^{\epsilon_P} \dot{P}_{15}^{\epsilon_{\dot{P}}}) + L_{\text{corr}}, \quad (2)$$

with  $L_0 = 0.18 \text{ mJy kpc}^2$ ,  $\epsilon_P = -1.5$ ,  $\epsilon_{\dot{P}} = 0.5$ .  $L_{\text{corr}}$  is a normally distributed random function with a zero average and  $\sigma_{L_{\text{corr}}} = 0.8$ .  $P$  is the spin period, and  $\dot{P}_{15}$  is the period derivative in units  $10^{-15} \text{ s s}^{-1}$ . The beaming fraction is calculated as in Faucher-Giguère & Kaspi (2006). A pulsar is detectable only above the death-line (Ruderman & Sutherland 1975; Rawley et al. 1986):

$$\frac{B}{P^2} > 0.12 \cdot 10^{12} \text{ G s}^{-2}, \quad (3)$$

where  $B$  is the equatorial magnetic field.

In all runs the number of objects used in the analysis is equal to 905, i.e. equal to the number of the data-points from the Parkes

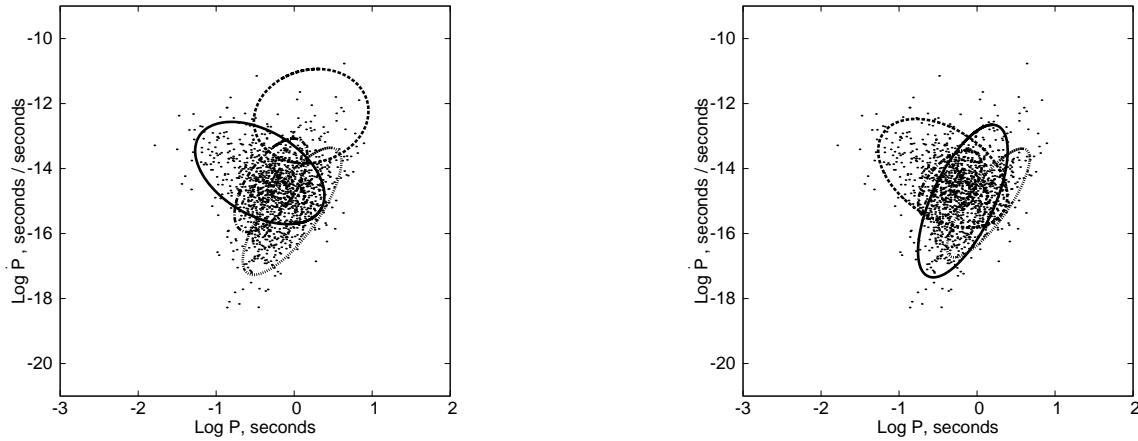


**Figure 2.** The same as Figure 1, but 10 per cent of the objects are randomly removed. The probability that the model and the data are drawn from the same parent distribution is 94 per cent for the model in the left panel, and 95 per cent for the model in the right panel.

**Table 1.** List of synthetic models.

Name	Fig.	Electron density	Prob.	Remarks
Model I.	4	NE2001	0.99	–
Model II.	5	$DM = 15D$	0.89	–
Model III.	6	NE2001	0.999	exp. decay (Eq. 5)
Model IV.	7	$DM = 15D$	0.96	no spiral arms
Model V.	8	$DM = 15D$	0.92	increased $R_{Gal}$
Model VI.	9	NE2001	0.94	bimodal in $P_0$
Model VII.	10	NE2001	0.97	bimodal in $B_0$
Model VIII.	11	NE2001	0.98	Popov et al. (2010), no decay
Model IX.	11	NE2001	0.96	Popov et al. (2010), decay

survey (see Fig. 3). The analysis based on the GMM appears to be dependent on the number of pulsars considered. Therefore, we decide to use the same number of pulsars in all generated samples as it is in the Parkes multibeam survey (see 3.1).

All models are listed in the Table 1, and short comments are given for each.

### 3.2.1 The simplest toy models

We start with the simplest models with the standard magneto-dipole losses with a constant angle between the spin and the magnetic dipole axis. The magnetic field is constant, too.

In the first model that we present, the electron density is calculated according to the NE2001 (Cordes & Lazio 2002). The data can be well described with four clusters, see Figure 4. Three clusters are rather similar to those we see in the fit for the Parkes multibeam survey data (Figure 3). The left cluster, containing just four pulsars, breaks this similarity. Note that this cluster is statistically significant. Indeed, the GMM finds no similar models with just three clusters. And the most probable model with three clusters is drawn from the same parent distribution as the data with the probability 92 per cent (compare with 99 per cent for 4 clusters).

The results presented in Figure 4 reproduce all main features seen in the plot for the Parkes data (Figure 3). However, slightly different runs of the population synthesis code, where the integration of the individual pulsar histories lasted not for  $3 \cdot 10^8$  yrs, but less, for example  $2 \cdot 10^8$  yrs, produce very different results in terms

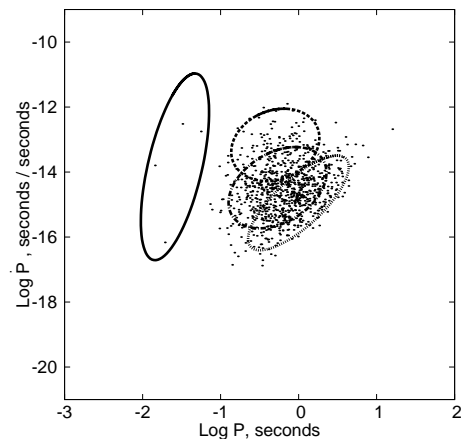


**Figure 4.** Model I. The magnetic field is constant. Pulsars are born in spiral arms. The electron density is calculated with the NE2001 model. The probability that the model and the data are drawn from the same parent distribution is 99 per cent.

of the identified clusters. In our opinion, this demonstrates that even for the simple models with well understood ingredients the method does not produce a stable set of easily interpretable clusters.

We can simplify the Model I by using a less complex model for the electron density distribution in the Galaxy. In the Model II, the dispersion measure is calculated with a simple relation:

$$DM = 15 D. \quad (4)$$

Here  $D$  is the distance in kpc. The minimum brightness is dependent on the interstellar scattering time,  $\tau_{scat}$ . If the  $DM$  is taken in the form (4), then  $\tau_{scat}$  is calculated according to Equation (7) from Lorimer et al. (2006).

If we compare Models I and II, the results are changed significantly. In the simpler model, only two clusters are necessary to describe the data, see Figure 5. We conclude that the effects connected with the fluctuations of the electron density are strong, and influence the number and the distribution of ellipses quite significantly.

In addition, we made calculations for the modified simplest Model IV when the electron density distribution is calculated according to NE2001. We do not present the figure, but the results

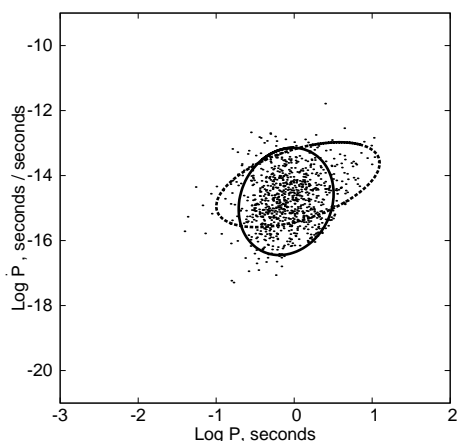


**Figure 5.** Model II. The same as Model I in Fig.4, but instead of the NE2001 model we use a simple linear relation between distance and dispersion measure (Eq. 4). The probability that the model and the data are drawn from the same parent distribution is 89 per cent.

are changed significantly. This again confirms that the influence of electron density distribution on the picture of gaussian clusters is essential.

In principle, the identification of just two clusters in a set of the observational data can lead to a conclusion of some dichotomy either in the initial properties or in the evolutionary laws. Here, obviously, the pulsars are born from a single mode population. The evolution also does not contain any process which can result in a dichotomy of sources. Therefore, the origin of such dichotomy is puzzling. We will simplify the model even more in Section 3.2.3 in an attempt to clarify it.

### 3.2.2 Field decay

Now we add to our scenario the magnetic field decay. The first model of this type (Model III) is similar to the one shown in Figure 4, but the field decays exponentially. For the illustrative purposes we choose a simple model:

$$B(t) = B_0 \exp \left[ -\frac{t}{\tau_{\text{mag}}} \right]. \quad (5)$$

Here  $\tau_{\text{mag}} = 5 \cdot 10^6$  years. We see (Figure 6), that the set of ellipses is very different from the Model I. In most cases the pulsars with larger  $\dot{P}$  are joined in one Gaussian with the pulsars from the main population, so it is difficult to identify if there is a magnetic field decay in this model, looking at the distribution of the ellipses.

### 3.2.3 Spatial distribution

Let us make further simplifications of the Model II presented in Figure 5. Now we exclude the spiral structure. This is the simplest model we study here (Model IV), see Fig. 7. The picture looks only slightly different.

Another modification related to the spatial distribution is very artificial. We want to study how the finite size of the Galaxy influences the picture. Therefore, we increase the size of the Galaxy,  $R_{\text{Gal}}$ , by a factor of three, and increase the pulsar production rate respectively. The results for the Model V are presented in Figure 8. Now the distribution is described with three clusters and two of them are elongated along the death-line.

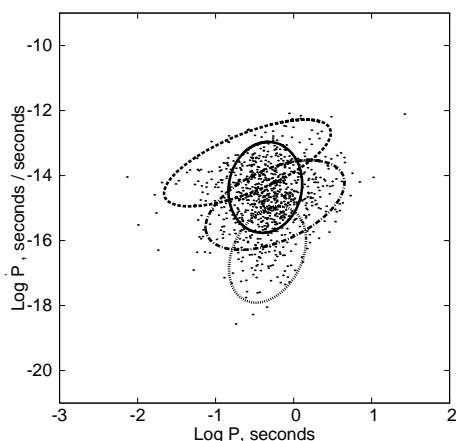


**Figure 6.** Model III. Similar to Model I, but the magnetic field decays exponentially. The probability that the model and the data are drawn from the same parent distribution is 99.9 per cent.

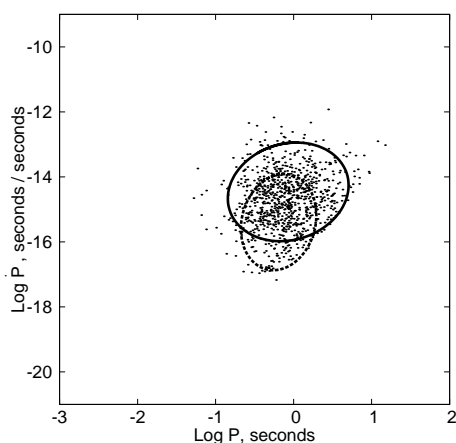


**Figure 7.** Model IV. Similar to Model II, but the birth places of the pulsars are not related to the spiral arms. The probability that the model and the data are drawn from the same parent distribution is 96 per cent.

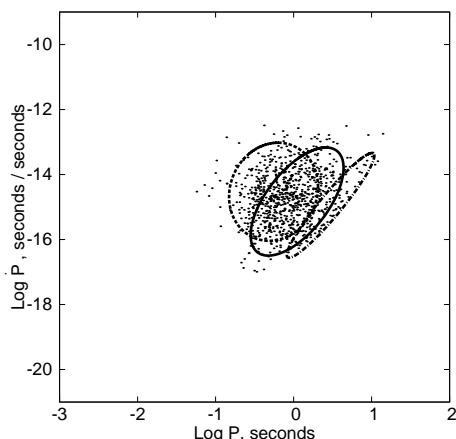


**Figure 8.** Model V. Similar to Model II, but the size of the Galaxy and the total birth rate are increased. The probability that the model and the data are drawn from the same parent distribution is 92 per cent.

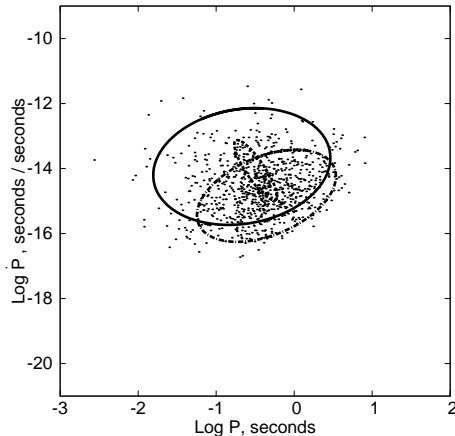


**Figure 9.** Model VI. The initial spin period distribution consists of two Gaussians:  $\langle P_0 \rangle = 0.02$  s,  $\sigma_P = 0.02$  s, and  $\langle P_0 \rangle = 0.2$  s,  $\sigma_P = 0.05$  s. The probability that the model and the data are drawn from the same parent distribution is 94 per cent.

### 3.2.4 Initial distributions

In this subsection we present two models with modified initial distributions of the spin periods and the magnetic fields. Instead of using a single Gaussian for each of these parameters, in one case we use two well-separated Gaussian distributions for the initial spin periods; in another we use two Gaussians for the magnetic fields (which are assumed to be constant during evolution).

In our Model VI the initial spin period distribution consists of two Gaussians:  $\langle P_0 \rangle = 0.02$  s,  $\sigma_P = 0.02$  s, and  $\langle P_0 \rangle = 0.2$  s,  $\sigma_P = 0.05$  s.

Three clusters are identified, see Figure 9. They overlap sufficiently. We suppose that for the GMM it is difficult to distinguish pulsars from different sub-populations because of their significant mixing. After a short time (about  $10^4 - 10^5$  years) pulsars with shorter periods are braked enough and can be confused with younger pulsars from the second sub-population with longer initial periods.

The picture of the clusters distribution for the case of the bimodal distribution of the initial magnetic field could look simpler as pulsars with stronger magnetic fields are higher in the  $P - \dot{P}$  plane, and they are never mixed with low-magnetized pulsars without the field decay. Nevertheless, in the case of two Gaussians for the initial magnetic field we have to make them very well separated to identify these groups using the GMM-code. When the first Gaussian is centred on  $\log B_0/[G] = 12.65$  and the second — on  $\log B_0/[G] = 13.2$  (both with  $\sigma_B = 0.55$ ), the GMM is not able to distinguish them. Even for  $\log B_0/[G] = 12.3$  and  $\log B_0/[G] = 13.2$  (both with  $\sigma_B = 0.35$ ) the method does not work well. Only when we take  $\log B_0/[G] = 11.8$  and  $\log B_0/[G] = 12.7$  with  $\sigma_B = 0.15$  (Model VII) the two groups are clearly described by different ellipses. However, in this case it was also easily visible by eye, see Figure 10. Note, that the additional clusters are also necessary to describe the data, similar to Model I.

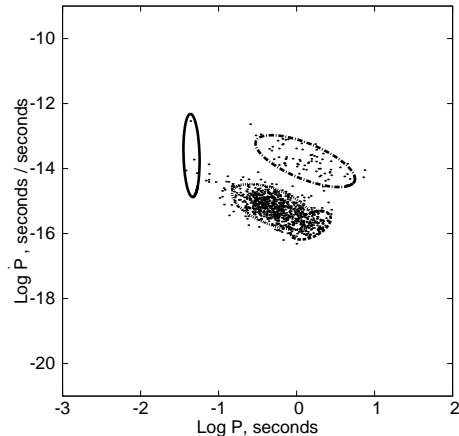


**Figure 10.** Model VII. The initial magnetic field distribution is bimodal:  $\log B_0/[G] = 11.8$ ,  $\sigma_B = 0.15$  and  $\log B_0/[G] = 12.7$ ,  $\sigma_B = 0.15$ . The probability that the model and the data are drawn from the same parent distribution is 97 per cent.

### 3.3 Analysis of the advanced synthetic models

It is interesting to apply the GMM to the results of the advanced models of the population synthesis. We use results of the calculations using the code of Popov et al. (2010)<sup>3</sup>.

We study two data sets: one with and one without the magnetic field decay. Both are fitted to reproduce the properties of the observed population. The results are presented in Figure 11. In the case of the constant field (Model VIII, left panel), the results can be described with just two clusters, as in the case of the most simple Model IV (Figure 7), but the ellipses have different properties. If the field is allowed to decay (Model IX), then we need three clusters. The ellipses now are clearly determined by the outlying points. The method does not distinguish the group of the initially higher magnetized pulsars which experienced significant field decay. Note, that in the original calculations no death-line was used, only the selection related to the flux, so no ellipse stretched along the death-line is seen. Note however, if we exclude points behind the death line, then the pictures is not changed significantly.

## 4 DISCUSSION

### 4.1 How effective is the Expectation-Maximization algorithm for the radio pulsars studies?

Based on the significant amount of numerical experiments we can conclude that the GMM method is not effective for the studies of normal radio pulsars. Let us try to speculate why this is the case.

The main initial distributions of pulsars in most of our models is defined by two Gaussians: one for the spin periods and the second — for the magnetic fields (in log-scale). However, the GMM method is applied to analyze the distributions in the  $P - \dot{P}$  not in the  $B - P$  plane. For the standard magneto-dipole braking ( $n = 3$ )  $\dot{P}$  can be expressed as:

$$\dot{P} = \frac{\alpha B^2}{P}. \quad (6)$$

<sup>3</sup> We thank prof. J.A. Pons for providing these data sets. Note, that the exact realisations used here are different from those presented in the paper by Popov et al. (2010).

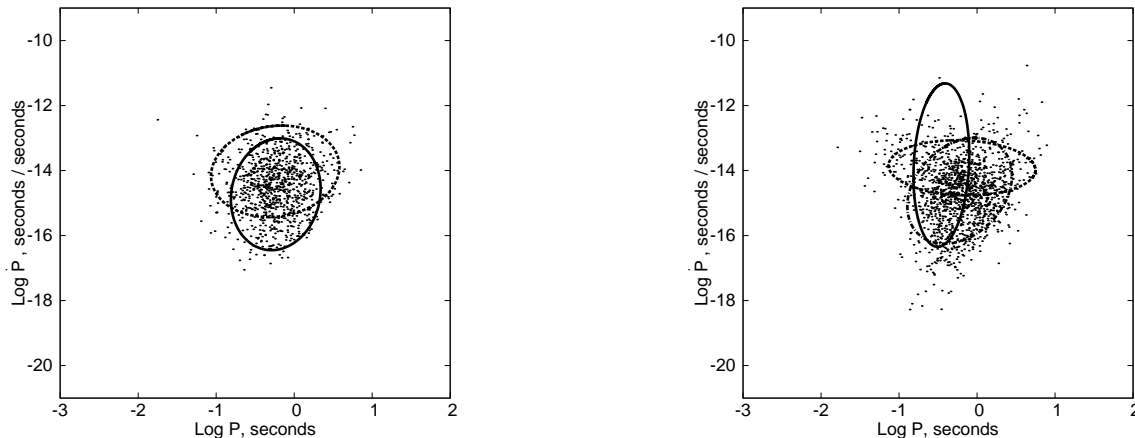


**Figure 11.** Models VIII (left panel) and IX (right panel). The data was calculated with the population synthesis model used in Popov et al. (2010). In the left panel pulsars evolve with constant magnetic fields. The K-S test probability for this model is 98 per cent. In the right panel results for decaying fields are presented. For this model the K-S test probability is 96 per cent.

Here  $\alpha = 8\pi^2 R^6 / (3Ic^3) = 10^{-39} \text{ cm s}^3 \text{ g}^{-1}$ ,  $R$  is the NS radius,  $I$  is the moment of inertia, and  $c$  is the speed of light. Therefore, the value of  $\dot{P}$  does not follow the Gaussian distribution (in log-scale or not) from the very beginning of our simulations. If the evolution does not follow the magneto-dipole formula the argument is also true for the models we used. In particular, it explains why the GMM method fails to describe with a single cluster the ensembles of pulsars when the maximum duration of the evolutionary track followed was short. For example, we performed the calculations for the maximum track duration equal to  $\sim 2 \cdot 10^7$  years. And in this case the results cannot be explained by a single cluster.

Simple replacement of  $\dot{P}$  by  $B$  does not improve the situation. Pulsars are rapidly evolving objects, and in the  $P - \dot{P}$  plane we can find objects at different stages of their evolution. The tracks of pulsars in the  $P - \dot{P}$  plane in the simple case of the constant effective magnetic field are straight lines. The length of the line is determined by the age, the initial spin period and the initial magnetic field. Therefore, the longer lines are in the upper part of the  $P - \dot{P}$  plot. During the evolution, the Gaussian distribution of pulsars in the  $P - B$  plane shifts and rotates. In addition to the already evolved pulsars, there are new ones being born constantly. Consequently, the distribution would not follow a Gaussian distribution even in the case of  $P - B$  plot.

L12 discussed the problem of robustness of the method in their study, too. The authors show that if 3 per cent of all pulsars are randomly removed from the dataset, no significant changes appear in the structure of the cluster distribution. In our opinion, 3 per cent is a small number. New observations routinely bring many tens, or even hundreds of newly discovered objects. So, 10 per cent is a more realistic number to study the stability of the method. It is shown above that a 10 per cent modification of the number of pulsars changes the results significantly. In addition, as we have demonstrated, a systematic exclusion of even a small number of objects (magnetars etc. in the studied case) also changes the set of the ellipses significantly. This brings us to the conclusion that the method is not very effective.

## 4.2 Other examples

In our opinion, the GMM is not very effective in distinguishing physically or evolutionary related groups when applied to rapidly

evolving populations observed with significant selection effects. That is why we decided to apply the method to more “stable” sets of data.<sup>4</sup>

First, we decided to use the GMM-code to study the well-known distribution of the gamma-ray bursts (GRBs) in the duration-hardness diagram. It is well established that there are at least two populations: the long soft and the short hard bursts (Klebesadel 1992; Kouveliotou et al. 1993). The duration and hardness of GRBs data are obtained from the BATSE 4B Gamma-Ray Bursts Catalog (Paciesas et al. 1999). We applied the GMM method to the distributions of bursts by logarithm of duration ( $t_{90}$ ) and by logarithm of hardness. The hardness is defined as

$$S = \frac{F_{100-300 \text{ keV}}}{F_{50-100 \text{ keV}}}, \quad (7)$$

where  $F_{100-300 \text{ keV}}$  is the flux in the energy range 100-300 keV, and  $F_{50-100 \text{ keV}}$  is the flux in the range 50-100 keV.

Naively, one expects that the method will easily describe the distribution with two clusters which correspond to the two GRB types. But this is not the case! In Figure 12 we see that the method requires four clusters. Depending on the initial guess, a different configuration of ellipses with nearly equal likelihood can appear, and in some of them the ellipses overlap.

For another test we choose the high-mass X-ray binaries, in particular the Be/X-ray systems. For these, the existence of two types have been established by Knigge et al. (2011). We want to check, whether the Expectation-Maximization algorithm can also identify this dichotomy. The data on Be/X-ray binary systems is taken from the catalog by Raguzova & Popov (2005)<sup>5</sup>.

The GMM method was applied to the distribution of Be/X-ray pulsars by logarithm of the spin period and the logarithm of the orbital period. The results are shown in Figure 13. Indeed, two Gaussians are enough to describe the data. However, we do not see that the method separates sources into long (both, the orbital and the spin) and the short periods. Instead, the short period sources are united with those with the longest periods. We have to note

<sup>4</sup> In L12 it was demonstrated that the method can be successfully used for the millisecond pulsars, which evolve much more slowly compared to the normal radio pulsars.

<sup>5</sup> The catalog is available on-line at <http://xray.sai.msu.ru/~raguzova/BeXcat/>

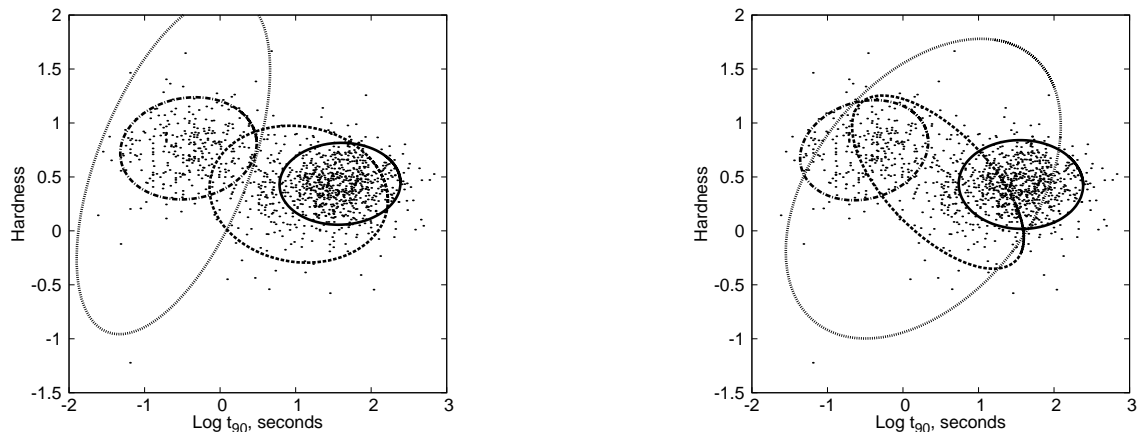


**Figure 12.** Gamma-ray bursts analysis. Two realizations of the Expectation-Maximization method are shown. In both cases, the well-known bimodal distribution in the duration-hardness cannot be described by two Gaussian clusters. The probability that the presented model and the data are drawn from the same parent distribution is 99 per cent for the model in the left panel, and 97 per cent for the model in the right panel.

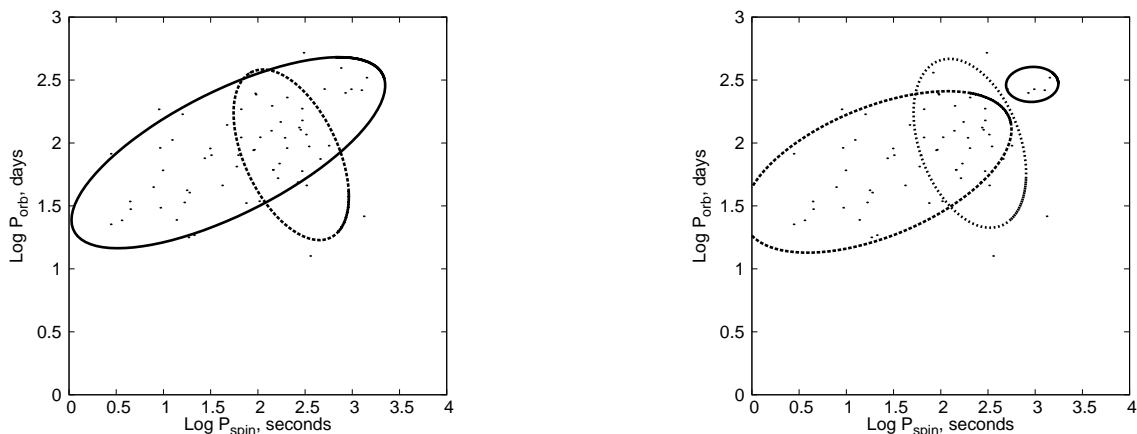


**Figure 13.** Analysis of the  $P_{\text{spin}} - \dot{P}_{\text{orb}}$  distribution of Be/X-ray binaries with the GMM method. The probability that the model and data are drawn from the same parent distribution is 99.9 per cent for both models.

here, that the objects with the longest periods that we use were not included in the sample in Knigge et al. (2011).

## 5 CONCLUSIONS

In our study, the GMM method was at first applied to the distributions of the known normal radio pulsars in the  $P - \dot{P}$  plane. It is found that the exclusion of magnetars, the thermally emitting NSs, etc. modifies the set of the clusters as compared to those found by L12. The pulsars detected in the Parkes multibeam survey may be described with just three clusters. It was also found that the results of the Gaussian cluster finding procedure are not robust (or the GMM method is oversensitive and the small changes in the data cause significant changes in the results). The relative position of the ellipses were changed when we excluded random 10 per cent of the pulsars from the observational data set.

In the second part of our study we generated ensembles of pulsars using population synthesis models of different complexity. First, we find that the GMM method is strictly dependent on the total number of pulsars in the analyzed ensemble. The choice of the electron density model also has a strong influence on the cluster distribution. The spiral structure of our Galaxy has a smaller effect.

Such features as the bimodal distribution of the initial parameters are hardly recognized by the GMM method for the realistic choices of parameters. The magnetic field decay changes the distribution of the clusters. Typically, if the field is decaying it is necessary to use more clusters to describe the data.

We conclude that the GMM is not effective to test models of the normal radio pulsar evolution because of the method's oversensitivity.

## ACKNOWLEDGMENTS

We thank Kejia Lee for numerous useful comments during the whole work on this study and on the text of the manuscript. Special thanks to Vasily Belokurov, who carefully read the paper which helped to improve its style. We also thank the referee for useful remarks and suggestions. The work of S.P. was supported by the RFBR grant 12-02-00186. The work of A.P. was supported by Saint Petersburg University grant 6.38.73.2011.

## REFERENCES

- Cordes J. M., Lazio T. J. W., 2002, arXiv: astro-ph/0207156
- Faucher-Giguère C.-A., Kaspi V. M., 2006, *ApJ*, 643, 332
- Hewish A., Bell S. J., Pilkington J. D. H., Scott P. F., Collins R. A., 1968, *Nature*, 217, 709
- Kim S. C., Kang T. J., 2007, *Pattern recognition*, 40, 1207
- Klebesadel R. W., 1992, in Ho C., Epstein R. I., Fenimore E. E., eds, *The durations of gamma-ray bursts Gamma-ray bursts - observations, analyses and theories*. Cambridge University Press, Cambridge, pp 161–168
- Knigge C., Coe M. J., Podsiadlowski P., 2011, *Nature*, 479, 372
- Kouveliotou C., Meegan C. A., Fishman G. J., Bhat N. P., Briggs M. S., Koshut T. M., Paciesas W. S., Pendleton G. N., 1993, *ApJ*, 413, L101
- Kuijken K., Gilmore G., 1989, *MNRAS*, 239, 651
- Lee K. J., Guillemot L., Yue Y. L., Kramer M., Champion D. J., 2012, *MNRAS*, 424, 2832
- Lorimer D. R., Faulkner A. J., Lyne A. G., Manchester R. N., Kramer M., McLaughlin M. A., Hobbs G., Possenti A., Stairs I. H., Camilo F., Burgay M., D’Amico N., Corongiu A., Crawford F., 2006, *MNRAS*, 372, 777
- Manchester R. N., Hobbs G. B., Teoh A., Hobbs M., 2005, *AJ*, 129, 1993
- Manchester R. N., Lyne A. G., Camilo F., Bell J. F., Kaspi V. M., D’Amico N., McKay N. P. F., Crawford F., Stairs I. H., Possenti A., Kramer M., Sheppard D. C., 2001, *MNRAS*, 328, 17
- Paciesas W. S., Meegan C. A., Pendleton G. N., 1999, *ApJS*, 122, 465
- Popov S. B., Pons J. A., Miralles J. A., Boldin P. A., Posselt B., 2010, *MNRAS*, 401, 2675
- Press W. H., Teukolsky S. A., Vetterling W. T., Flannery B. P., 2007, *Numerical recipes: the art of scientific computing*. Cambridge University Press, Cambridge
- Raguzova N. V., Popov S. B., 2005, *Astronomical and Astrophysical Transactions*, 24, 151
- Rawley L. A., Taylor J. H., Davis M. M., 1986, *Nature*, 319, 383
- Reynolds D. A., Quatieri T. F., Dunn R. B., 2000, *Digital signal processing*, 10, 19
- Ruderman M. A., Sutherland P. G., 1975, *ApJ*, 196, 51
- Vallée J. P., 2005, *AJ*, 130, 569
- Vivekanand M., Narayan R., 1981, *Journal of Astrophysics and Astronomy*, 2, 315
- Vranesević N., Melrose D. B., 2011, *MNRAS*, 410, 2363